

Geology and mineralogy of Fe-Sn deposit in Batubesi, Belitung Island, Indonesia

Rudarsko-geološko-naftni zbornik (The Mining-Geology-Petroleum Engineering Bulletin) DOI: 10.17794/rgn.2025.5.7

Original scientific paper



Aryo Dwi Handoko¹¹²* ♠ ☒, Mochamad Slamet Sugiharto³ ☒, Syafrizal⁴ ♠ ☒, Alfend Rudyawan¹ ☒, Benyamin Sapiie¹ ☒

- Department of Geological Engineering, Faculty of Earth Sciences and Technology, Institut Teknologi Bandung, Indonesia.
- ² Research Center for Geological Resources, National Research and Innovation Agency, Indonesia.
- ³ PT TIMAH, Indonesia.
- ⁴ Department of Mining Engineering, Faculty of Mining and Petroleum Engineering, Institut Teknologi Bandung, Indonesia.

Abstract

Batubesi deposit is a primary Fe-Sn deposit located in the eastern part of Belitung, Indonesia. Previously, mineralisation was known as greisen, but recent studies show that the region has developed skarn-type deposits. Despite that, skarn-type mineralisation has not been well studied. This research aims to study Fe-Sn mineralisation in Batubesi with a geological and mineralogical approach, primarily from field observation and diamond drill core logs and samples. The laboratory methods used are petrology, SEM-EDX, micro-XRF, and XRD analysis to determine mineralogical assemblage, as well as fused bead XRF to determine the geochemical composition of the deposit. The results show that the Batubesi deposit is dominated by skarn-type mineralisation with minor greisen. Two skarn stages have been observed: prograde and retrograde. Prograde stages are characterised by the precipitation of calc-silicate minerals and magnetite then often fractured or brecciated. The fractures and breccia are then altered by the retrograde stage, composed of amphibole, muscovite, and biotite. Sometimes, the alteration is so intense that the previous prograde stage is completely altered. Furthermore, the retrograde stage consists of sulfide minerals as veins such as pyrite, chalcopyrite, and arsenopyrite. Magnetite is the common ore mineral, followed by cassiterite, scheelite, ferberite, pyrite, chalcopyrite, arsenopyrite, glau-cocerinite, and sphalerite.

Keywords:

Batubesi, iron-tin, skarn, ore deposit, mineralogy

1. Introduction

Tin is a critical metal for low-carbon technology (Moss et al., 2013) and other purposes, such as chemicals, tinplate, solder, and alloys (U.S. Geological Survey, 2022). Tin consumption has risen in the last two decades, primarily by increased consumption in China. The consumption increases also led to a shift in world tin consumption that changed the biggest tin consumers from Europe and North America to China (Li et al., 2021).

Historically, there are several critical tin-producing regions in the world, namely the Southeast Asian Tin Belt, South China Tin Province, the Central Andean Tin Belt, and Cornwall Tin Province (Lehmann, 2020). The Southeast Asia Tin Belt stretches from Myanmar to Indonesia through Thailand and Malaysia. This region is currently one of the significant tin mine areas that hosted

one-third of the estimated annual tin production in 2021 (U.S. Geological Survey, 2022).

Tin deposits can be classified into several categories

Tin deposits can be classified into several categories, such as pegmatite, greisen, porphyry, skarn, vein, and placer, with cassiterite as the main ore mineral (Dill, **2010**). Ionic radius of tin (Sn⁴⁺, 0.71 Å) is similar with iron (Fe³⁺, 0.64 Å), titanium (Ti⁴⁺, 0.68 Å), niobium (Nb⁵⁺, 0.70 Å), tantalum (Ta⁵⁺, 0.73 Å), and scandium $(Sc^{3+}, 0.81 \text{ Å})$ (Railsback, 2003). Thus, it can be substituted by those ions in earth-forming or other minerals. Garnet, an abundant mineral in skarn, can contain up to 1% tin, while magnetite in skarn deposits can incorporate up to 0.4% tin (Chen et al., 2022). Tin mineralisation source is believed from the breakdown of tin-bearing minerals such as muscovite or biotite caused by melting or alteration (Chen et al., 2022; Kunz et al., 2022; Wolf et al., 2018; Zhao et al., 2022). Additionally, tin may be preserved in magma and deposited in granite, increasing its content in granite (Neymark et al., 2021).

Skarn here is defined as mineralisation that contains an abundant amount of calc-silicate minerals, such as

Received: 5 March 2025. Accepted: 14 May 2025.

Available online: 21 October 2025

^{*} Corresponding author: Aryo Dwi Handoko e-mail address: 32020004@mahasiswa.itb.ac.id; aryodwihandoko@gmail.com

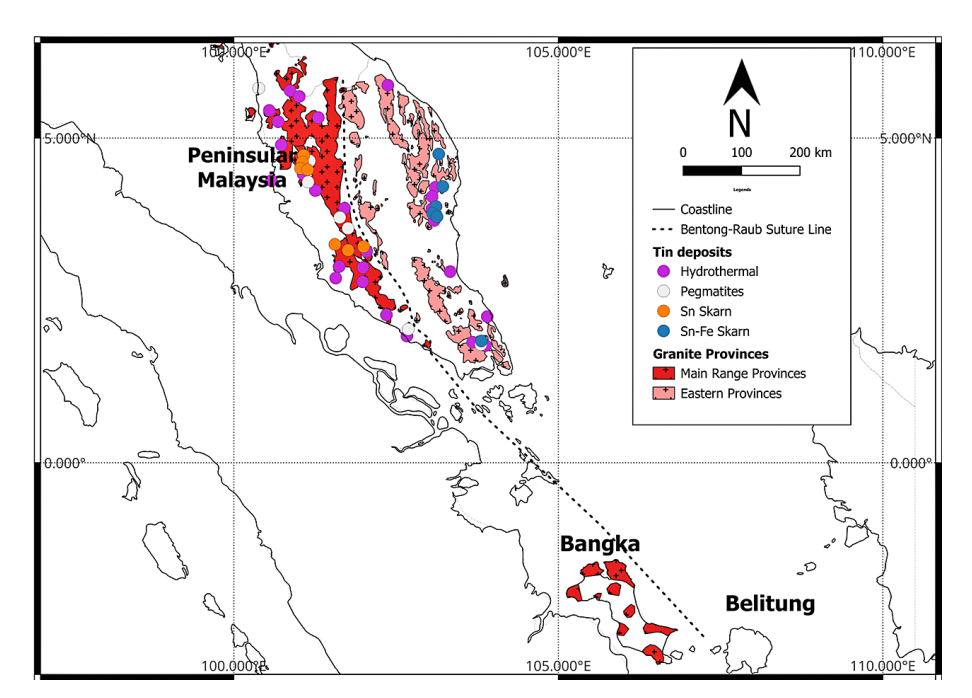


Figure 1. Maps of Peninsular Malaysia including Bangka and Belitung Islands, that show the spatial difference between Sn skarn (orange dot) and Sn-Fe skarn (blue dot). Tin deposits, Peninsular Malaysia granite provinces and Bentong-Raub Suture line from previous published data (Yang et al., 2020). Similarly, Bentong-Raub Suture line in oceans and Bangka granite provinces from published data (Ng et al., 2017).

garnet, pyroxene, and or wollastonite (Einaudi et al., 1981; Meinert, 1992; Meinert et al., 2005), hence its protolith may be other than carbonate rocks such as siliciclastic, igneous, or metamorphic rocks (Chang et al., 2019). Skarn can be subclassified based on their dominant metallic content, such as Cu-, Au-, W-, Sn-, and Fe-skarn (Meinert et al., 2005). Those skarns share similar compositional characteristics, such as Au, Mo, and W skarns commonly hosted in reduced skarn, meanwhile Cu skarns hosted in oxidised skarns (Meinert, 2020; Meinert et al., 2005). Besides that, skarn is also commonly zoned both temporally and spatially caused by variations of temperature and composition that also affect mineralisation patterns in skarn (Meinert, 1997). This zonation also affects garnet and pyroxene, common minerals in skarns. Furthermore, their ratio is controlled by redox conditions, which are regulated by magma and wall rocks, i.e. garnet is more abundant in more oxidised parts of the system (near intrusions), whereas pyroxene is more abundant in more reduced parts of the system (near wallrock) (Chang et al., 2019).

Primary tin mining in Belitung has been done in several deposits, such as Kelapa Kampit, Nam Salu, Tikus, Tebrong, and Selumar, with several other known tin mineral deposits (Adam, 1960; Crow & Van Leeuwen, 2005; Schwartz et al., 1995; Schwartz & Surjono, 1990). Batubesi is one of the known tin mineral deposits in Belitung, which was mined for its iron content and is currently being explored for tin mining. Historically, tin mineralisation types in Batubesi were known as vein and greisen (Schwartz et al., 1995; Sujitno et al., 1981). However, recent studies suggest that Batubesi tin mineralisation type is a skarn deposit (Bargawa et al., 2023; Sugiharto et al., 2024). Those studies mainly cover ore potency evaluation and tungsten occurrence with minimal detailed geological and mineralogical condition re-

lated to Fe-Sn skarn mineralisation in Batubesi explained. This study wants to emphasize and determine the geological and mineralogical characteristics of Batubesi skarn tin mineralisation. Additionally, this study wanted to present how skarn deposit can develop in Belitung Island where carbonate is not known to exist.

1.1. Geology of Belitung Island

Southeast Asia Tin Belt granite provinces can be divided into Main Range Province, Eastern Province, Western Province, and North Thailand Migmatitic Province (Cobbing et al., 1986) with different tin mineralisation type and metal association (Hutchison, 1978). Main Range Province and Eastern Province are divided by Bentong-Raub Suture, which also occurs as a boundary in tin skarn characteristics (Searle et al., 2012). It can be seen clearly in the Malay Peninsula, where tin skarn is mostly located in Main Range Province (western part of Bentong-Raub Suture), while tin-iron skarn is mostly located in Eastern Province (eastern part of Bentong-Raub Suture) (Yang et al., 2020) (see Figure 1).

Belitung Island is in the southern part of the Southeast Asian Tin Belt, located around the Bentong-Raub Suture zone, but the suture itself remains unclear. Some researchers argue that the suture developed from Malay Peninsula and extended to Belitung Island (Hutchison, 2014; Ng et al., 2017), while others claim that the suture is located in the southern Bangka and Belitung (Metcalfe, 2017; Searle et al., 2012). It is believed that Belitung is a peneplain area with resistive quartz standing as hills (Johari, 1987) with elevation commonly below 100m, with the highest point around 500m. Belitung is composed of siliciclastic sediments in which some of them undergone metamorphism, chert, basaltic lava, flysch sediments, and volcanic breccia intruded by grani-

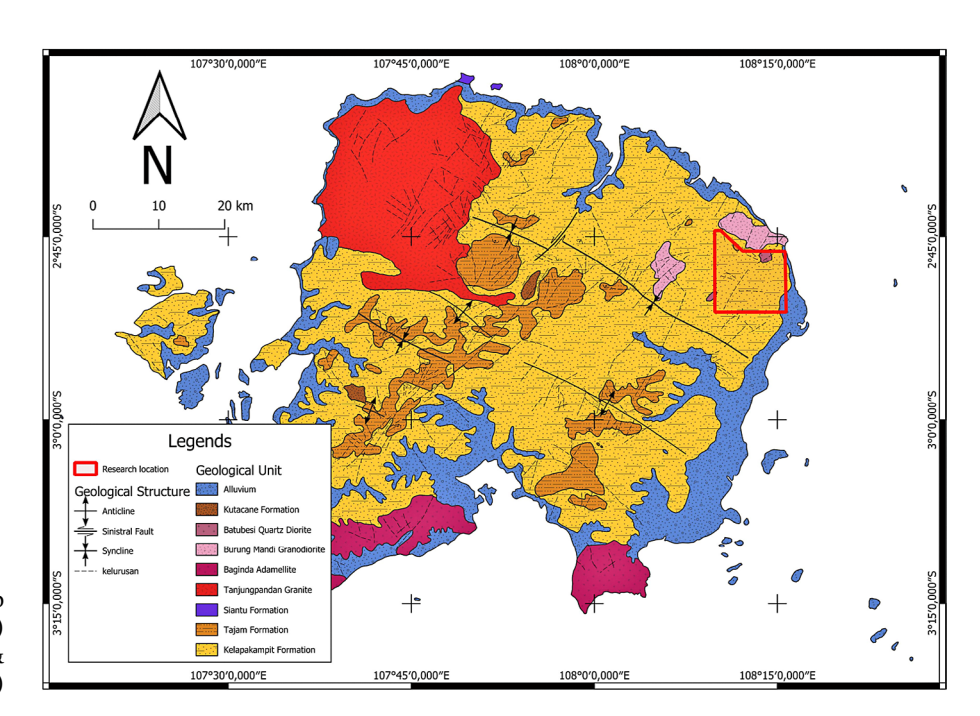


Figure 2. Belitung geological map with research location (red box) (modified after Baharuddin & Sidarto, 1995)

toid and diorite (Baharuddin & Sidarto, 1995). Flysch sediment fossils suggest that the rocks formed at the Permo-Carboniferous age in marine environments, similar to interfingering basaltic lava and volcanic breccia. Meanwhile, siliciclastic sediments probably interfingers flysch sediments but with unknown depositional environments. The sediments were then intruded by Tanjungpandan granite at 208-245 Ma, followed by Baginda Adamellite (160-208 Ma), Burungmandi Granodiorite (115-160 Ma) and Batubesi Quartz Diorite (115-160Ma) (Priem et al., 1975). Plutonic igneous rocks in Belitung can be divided into four types, namely gabbroic, granodioritic, adamellitic, and granitic rocks (Aleva, 1960). However, later studies suggest that no gabbroic igneous rocks are present; only basaltic lava can be found (Baharuddin & Sidarto, 1995).

1.2. Deposit geology

Batubesi Fe-Sn skarn deposit is one of the primary tin deposits located in Belitung Island, Indonesia. It is currently being explored for its tin mining potential, in continuation of previous iron mines. It is in the island's eastern part, approximately 20 km southwest of Open Pit Nam Salu Geosite. The elevation is around 12 to 25 meters with plain relief, close to Mang Mountain (406 m) and Bolong Mountain (305 m). The Batubesi Fe-Sn deposit is located at the contact between Kelapa Kampit flysch sediments (mostly siliciclastic) and granitic intrusions with a width of several hundred meters (see **Figure 2**).

2. Materials and methods

Three diamond drill cores and outcrop analysis have been performed to understand the rock, minerals, and alteration characteristics from the study area. Furthermore, seventy-eight rock samples from diamond drill cores have been collected to be analyzed for their mineral assemblage, geochemistry, and sequence in the laboratory. Most of the samples are taken from oriented drill cores, and their orientation is preserved in the samples. Handheld XRF was used in screening process to identify tin and metal rich samples but not displayed here as it only shows semi-quantitative results from the samples not reflecting their whole rock geochemistry. Several methods are used for analysis, such as petrography, SEM-EDX, micro-XRF, and X-ray diffraction. Some samples have undergone several analyses to ensure their mineral, texture, and structure identification process.

2.1. Petrography

Seventy-eight thin sections and eighteen polished samples have been analysed for their mineral, texture, and structure identification. One oriented diamond drill core sample may have several thin sections with different orientations. This method is best suited to determine mineral texture and structure that can determine mineral paragenetic sequences. Moreover, this method can be used to complement other mineral identification techniques. Polished sections were made when samples had substantial amounts of opaque minerals, some of which were also used for SEM-EDX and micro-XRF analyses. Polished samples taken from diamond drill cores were then mounted in resin and polished with diamond paste. The analysis was done at Faculty of Earth and Science and Technology, Institut Teknologi Bandung and National Research and Innovation Agency, Indonesia.

2.2. SEM-EDX

Four polished samples were analyzed for SEM Jeol JSM IT300 equipped with EDX Oxford XMAX at Ad-

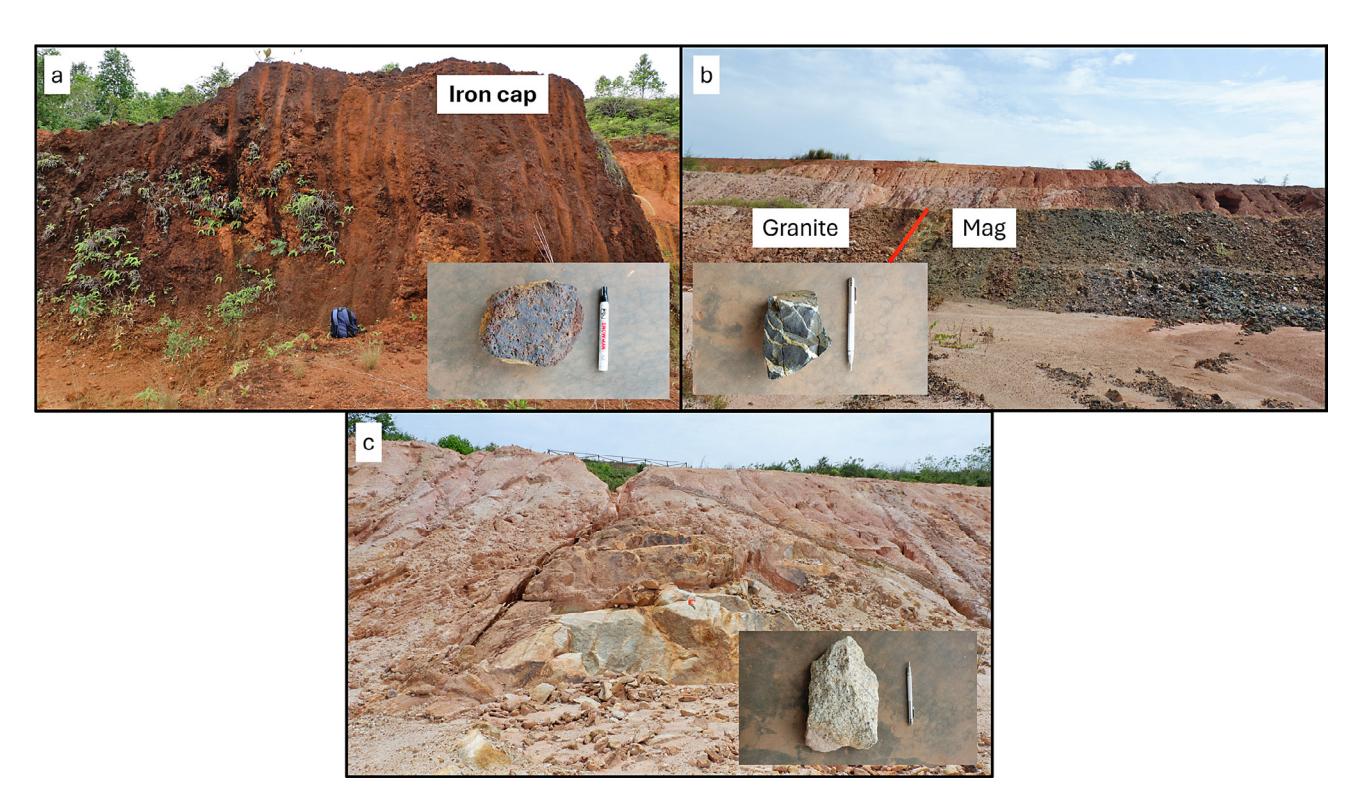


Figure 3. (a) Iron cap with vesicular structure (inset), commonly found near surface. (b) Contact between granite and magnetite-rich rocks (Mag) from pit bench. Magnetite commonly intruded by quartz vein (inset). (c) Granite outcrop in Batubesi with its hand specimen (inset). Abbreviations: Mag: magnetite

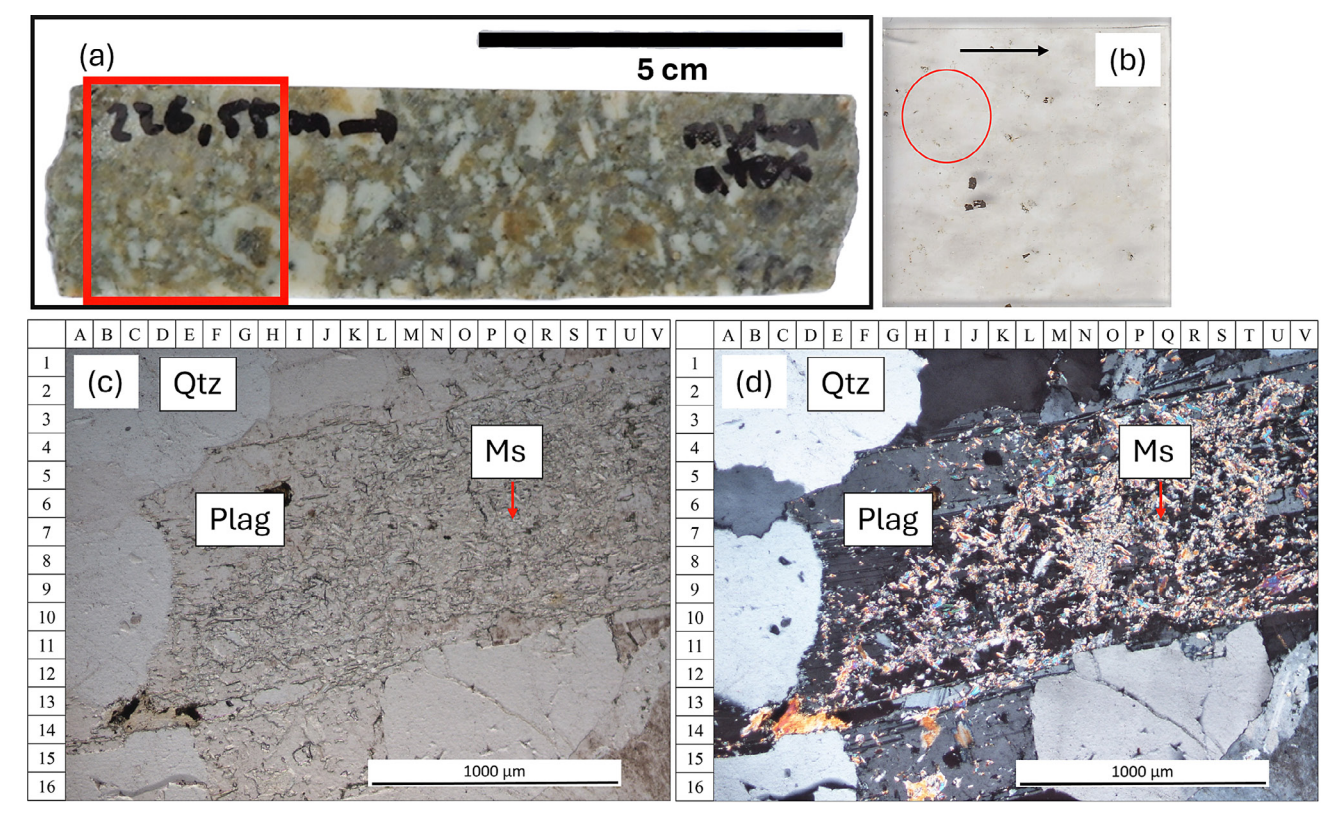
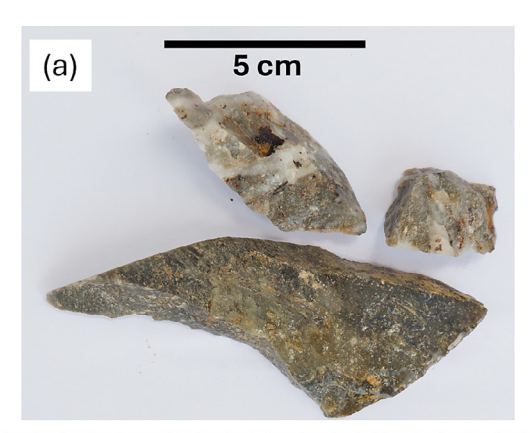


Figure 4. Photomicrograph of slightly greisenized granite shows plagioclase altered to muscovite from sample AB01020_A. Sample taken from drill cores marked with thin section region (red rectangle) (a), thin section marked with observation zone by optical microscope (red circle) (b), photomicrograph of observation zone in parallel nicol (c) as well as cross nicol (d). Abbreviations: Plag: plagioclase, Ms: muscovite



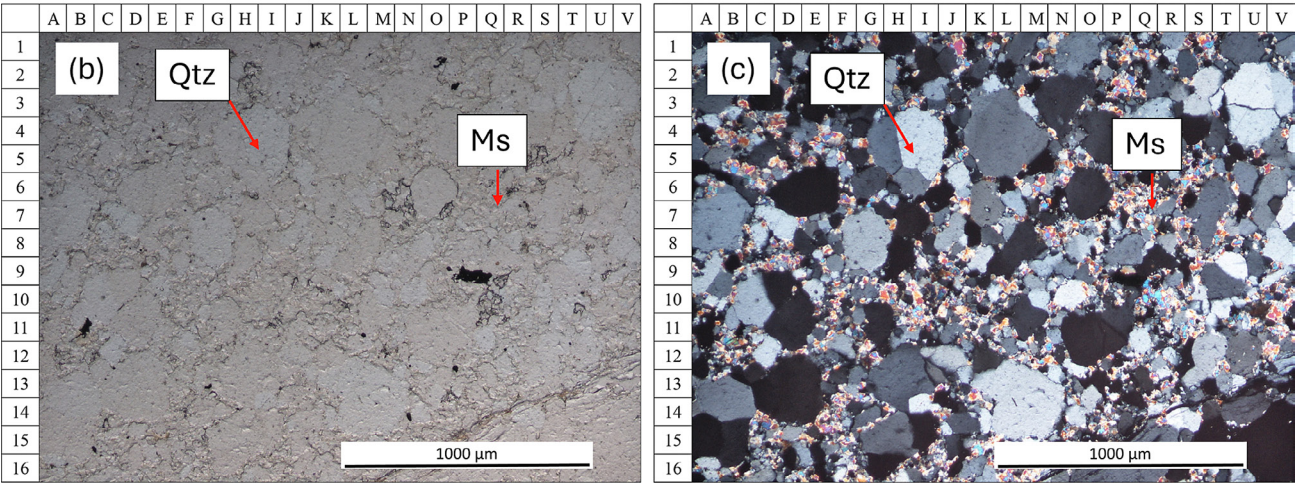


Figure 5. Sample taken from drill cores (a) with photomicrograph of greisen alteration in Batubesi in parallel nicol (b) as well as cross nicol (c) from sample AB01018_A. Greisen alteration near granitic rock marked by quartz (white-grey, H₅) (c) and muscovite (high birefringence, III) (c) rich rocks. Abbreviations: Qtz: quartz, Ms: muscovite

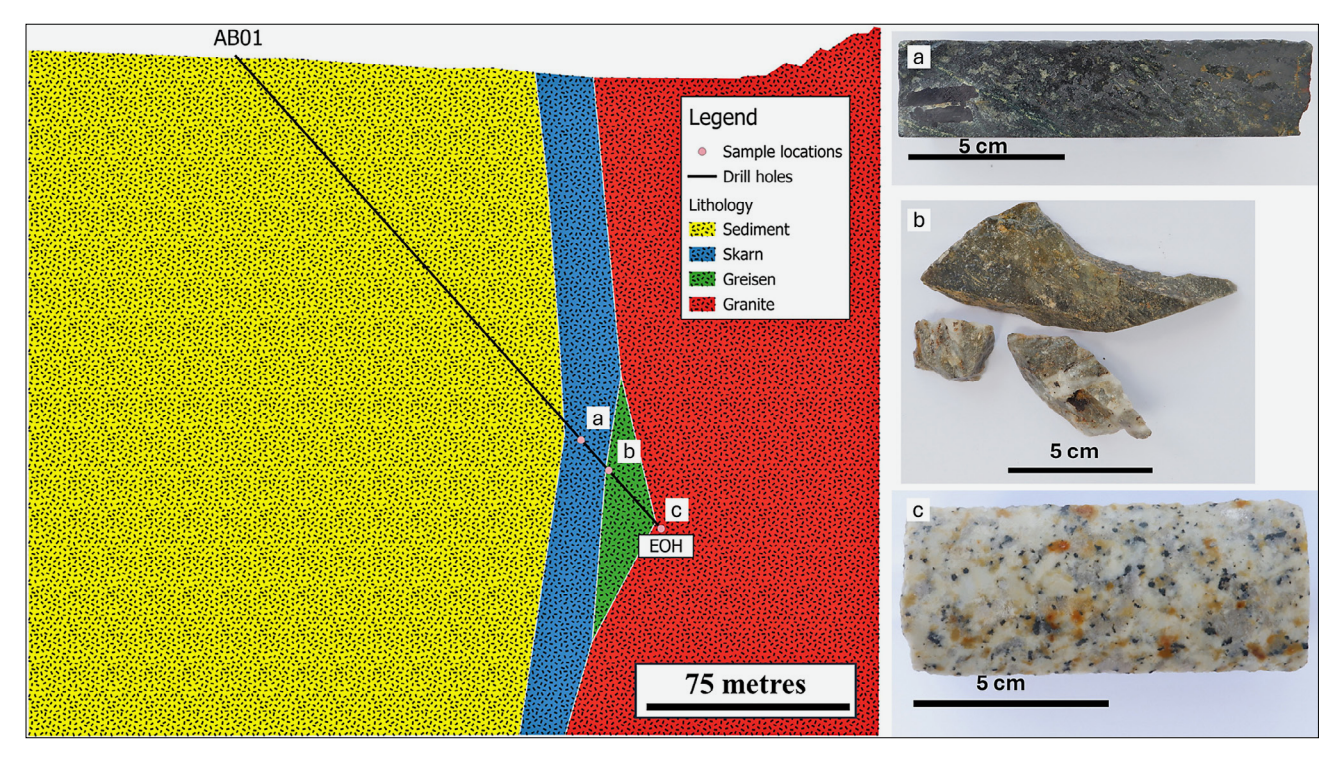


Figure 6. A cross-section of ABo1 from Batubesi Fe-Sn deposit shows the relative position of granite, greisen, skarn, and sedimentary rocks. Greisen (green) is located between granite (red) and skarn (blue)

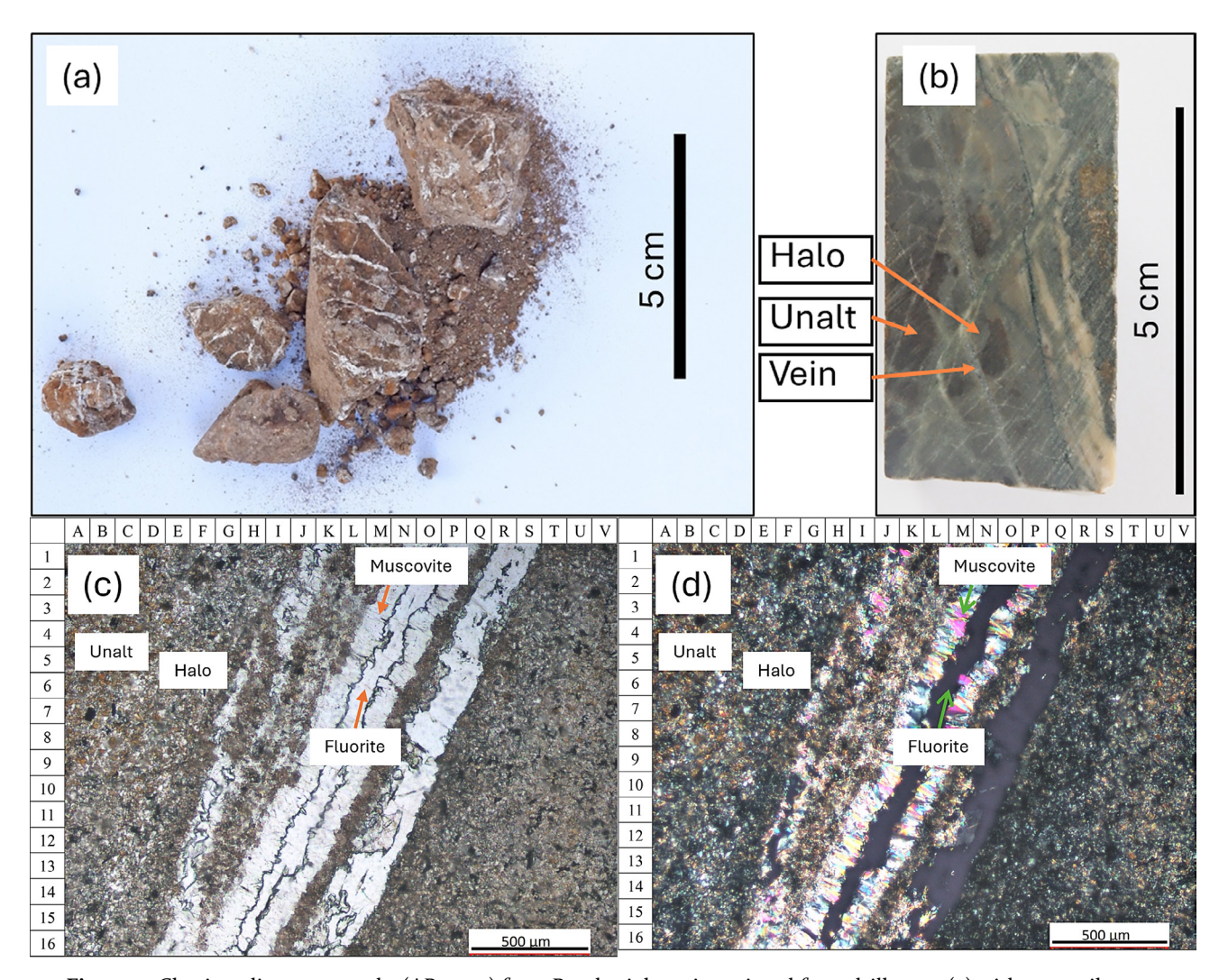


Figure 7. Clastic sedimentary rocks (AB01003) from Batubesi deposit retrieved from drill cores (a) with meta-siltstone (AB03006_B) (b) samples displaying unaltered meta-siltstone (Unalt), veins (Vein), and alteration halo around veins (Halo). Photomicrograph of meta-siltstone samples in parallel nicol (c) and cross nicol (d) shows the unaltered meta-siltstone, alteration halo, with fluorite-muscovite veins

vanced Characterization Laboratories Bandung, National Research and Innovation Agency, Indonesia. This method is used to determine minerals that contain light elements (e.g. fluorite). Samples are taken from petrographic polished sections that contain various types of opaque minerals as well as a high amount of tin. The sample numbers were then reduced that amount for various types of rocks and mineralisation. The samples are polished with diamond paste. Thus, some carbon contamination is expected during analysis. Samples were coated with gold before elemental mapping and elemental point analysis.

2.3. Micro-XRF

Five diamond drill samples were analyzed using Bruker M4 Tornado Plus micro-XRF analysis and AMICS to determine the mineral types based on their chemical composition. The samples were chosen based on their mineral characteristics as well as initial geochemical properties based on handheld XRF to describe important mineral-

ogical and geochemical characteristics of the deposit. The samples were analysed at Mineral Testing Laboratory Jakarta, National Research and Innovation Agency, Indonesia. Samples were analyzed with a pixel size of around 25-40 µm and pixel time between 15-25 ms/pixel.

2.4. XRD

Sixteen diamond drill samples were analyzed with powder X-ray diffraction at National Research and Innovation Agency, Indonesia. The samples have been chosen to analyse minerals that contain small minerals or texture that are hard to observe by optical microscopy. This method also serves as secondary analytical procedures to confirm petrographic and micro-geochemical analysis such as micro-XRF and SEM-EDX. Samples were grounded manually to size below 200 mesh with agate mortar and pestle to retain their mineral structure. They were analyzed by CuKα X-ray source with 5°-90° 2-theta angles. The spectra are then compared with an open X-ray spectra database (e.g. Lafuente et al., 2016).

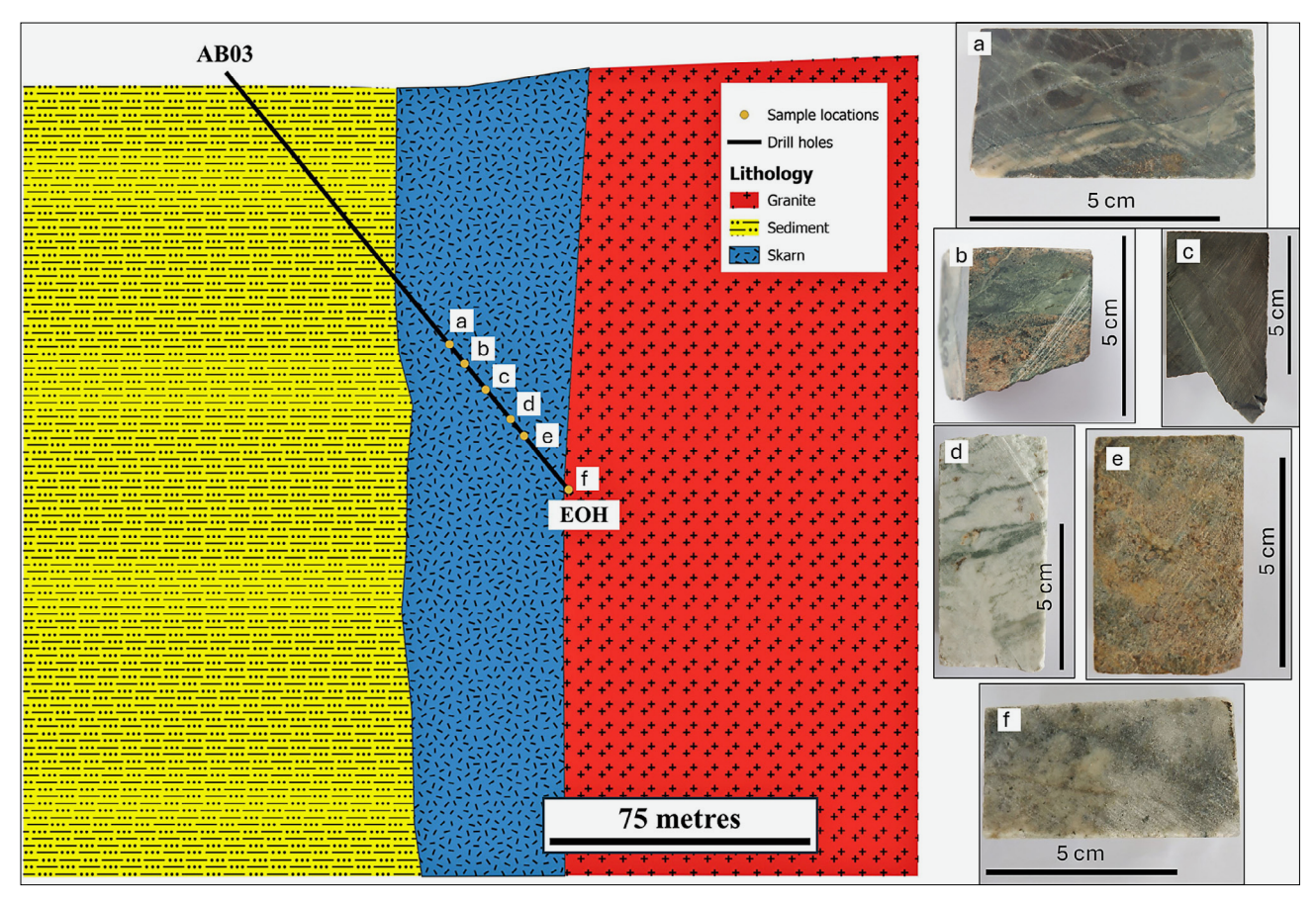


Figure 8. A cross-section of ABo3 from Batubesi Fe-Sn deposit shows the relative position of skarn mineralisation with granite and sedimentary rocks. Siltstone (a, c) are located between garnet mineralisation, whereas wollastonite-rich rocks (d) are located within the skarn mineralisation

3. Results

Batubesi Fe-Sn deposit is located in a flat area and has been mined with open pit methods, resulting in tens of meters deep holes and some of them submerged below the water surface. Besides that, near Batubesi mines, there are several abandoned small holes from artisanal tin mining filled with water. At the top part of the deposit, iron caps composed of vesicular magnetite are observed (see **Figure 3a**). These vesicular rocks are also commonly found as boulders around the deposit with various sizes around tens of centimetres.

Fresh rock outcrops are scarce outside the open pit, and the surrounding ground is mixed with materials from previous mining, which hinders rock identification based on weathered materials. Skarn mineralisation was identified as black magnetite-rich rock intruded by quartz veins that can be found around open pit floor and bench (see **Figure 3b**). Besides that, granitic rocks are also found in the open pit bench with fractures commonly developed on it (see **Figure 3c**).

Three-stage skarn mineralisation has been observed in the study area: isochemical metamorphism, prograde and retrograde. Isochemical metamorphism is characterised by the occurrence of meta-siltstone in Batubesi deposit. The prograde stage is dominated by magnetite and



Figure 9. Wrigglite textures with black and white bands cut by veins in the shallower part of the deposit. SEM-EDX and petrographic analysis show that the black bands are magnetite with small amounts of cassiterite and wolframbearing minerals, while the white bands are fluorite.

calc-silicate mineralisation, e.g. garnet, pyroxene, vesuvianite, and wollastonite. Magnetite-garnet are the main minerals in highly altered regions, where almost all host rocks are altered, and their texture is not visible. Magnetite can be found in massive, banded, or veins and sometimes have rhythmically altered bands with arsenopyrite. Magnetite was observed being cut by carbonate and quartz veins. Conversely, garnet commonly occurs in massive texture along with fluorite and is often brecciated or fractured and then filled with biotite, muscovite, and amphibole minerals from the retrograde stage. It is also cut by other minerals from retrograde stage such as quartz, Fe-oxides (hematite), and carbonate

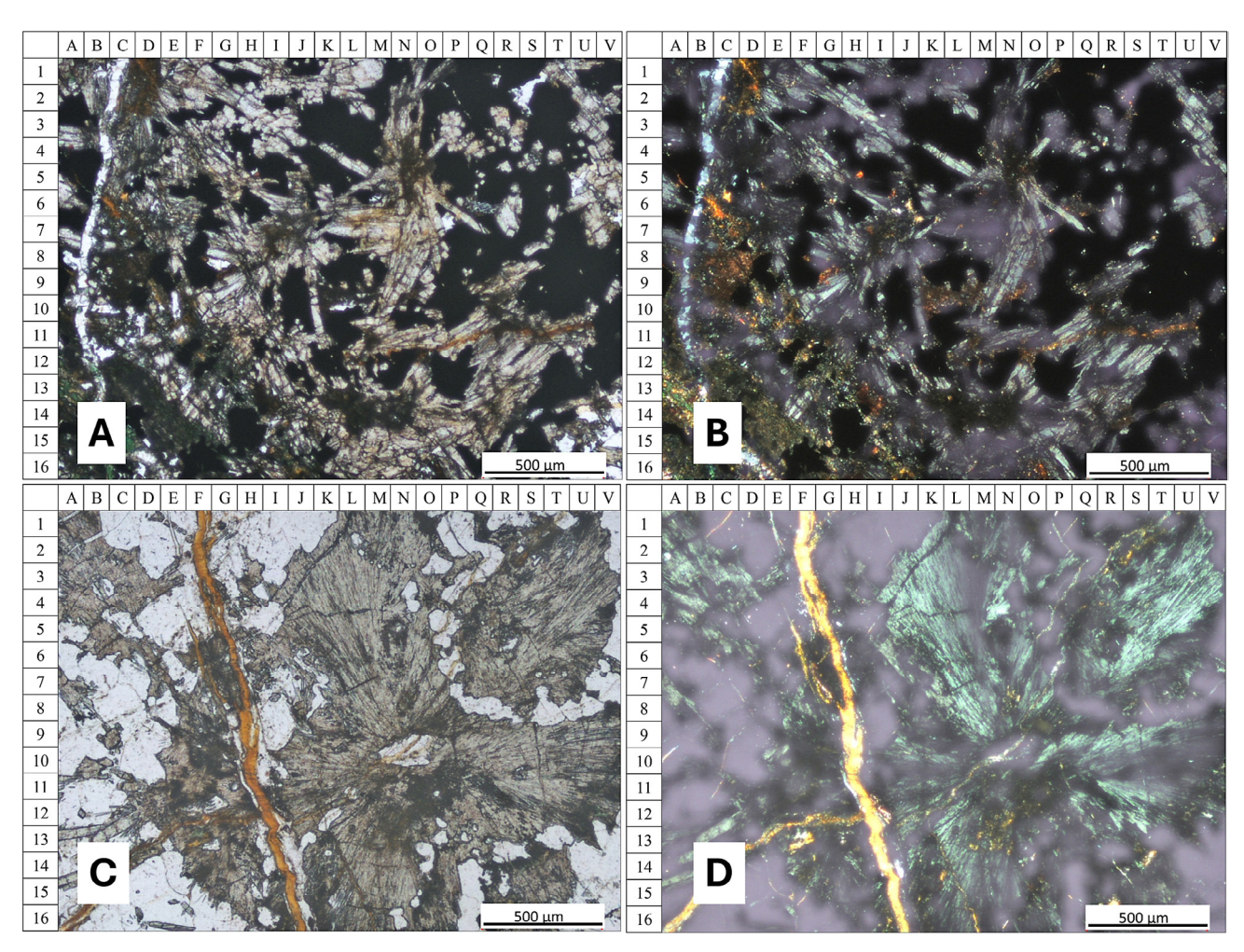


Figure 10. Photomicrograph of skarn sample from ABo2015_A shows magnetite and garnet infill and cut host rock minerals with parallel nicol (a, c) and cross nicol (b, d) polarization, respectively. Magnetite (black, J10) (a) infills the space between chalcedony (white-grey, H10) (a) and cuts by quartz vein (white, C1) (a). Cross nicol (b) shows magnetite as black (J10), while chalcedony as greenish grey (H10) with biotite as reddish brown (B6). Moreover, in cross nicol (d), garnet (black, P5) cut radial chalcedony (green-grey, S5), then both cut by later vein (yellow, F1). Parallel nicol (c) show garnet as white-grey (P5) and chalcedony as grey (S5).

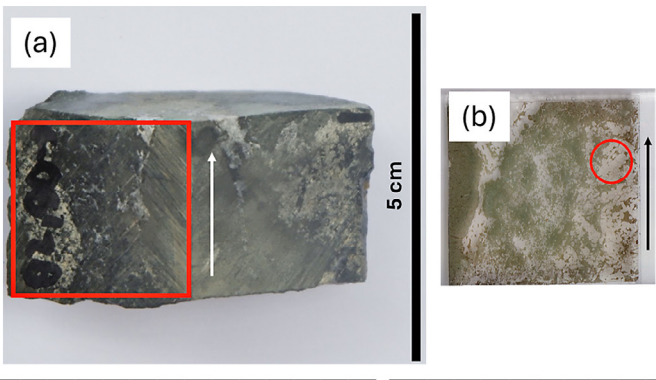
veins with or without an alteration envelope. Additionally, the retrograde stage also consists of sulfide minerals such as pyrite, chalcopyrite, and arsenopyrite

3.1. Petrology and mineralogy

Granitic rocks in the area are fine-grained, equigranular to porphyritic rocks mainly composed of quartz and feldspar, minor biotite and trace amounts of zircon. Many of them are greisenized from slightly altered (see Figure 4) to moderately altered (see Figure 5). Greisen alteration occurs near the contact between granitic rock and host rock, marked by quartz and muscovite-rich rocks, sometimes with chlorite-muscovite veins cutting through it (see Figure 6) or replacing plagioclase (see Figure 4). Muscovite is usually found between quartz minerals with a size of around 40 µm. Alteration intensity is reduced when moving away from the magnetite-garnet zone and is characterised by the absence of magnetite; only garnet exists, and the more unmineralised host rock is present. Wollastonite mineralisation occurs

in these lower-intensity alteration zones that are several meters thick. Additionally, Fe-oxide minerals are dominated by hematite near the surface.

The host rocks in the Batubesi deposit contain friable clastic sedimentary rocks that can be observed from drill cores, and it does not contain carbonate (see Figure 7a). Near the granite-host rock contact, the host rock has undergone metamorphism and is mainly observed as metasiltstone. It has a black appearance with a gritty texture that can absorb water. Mineral size in meta-siltstone is small (around 12-34 µm) and difficult to distinguish by petrography analysis. However, X-ray diffraction analysis suggests that it comprises quartz, muscovite, and kaolinite. Meta-siltstones are commonly fractured, and veins of quartz, carbonate, muscovite, fluorite, and or chlorite are commonly found with or without an alteration halo (see Figure 7b). The metamorphosed rocks are also commonly found around minerals formed by the skarn process (e.g. calc-silicate and magnetite) (see Figure 8).



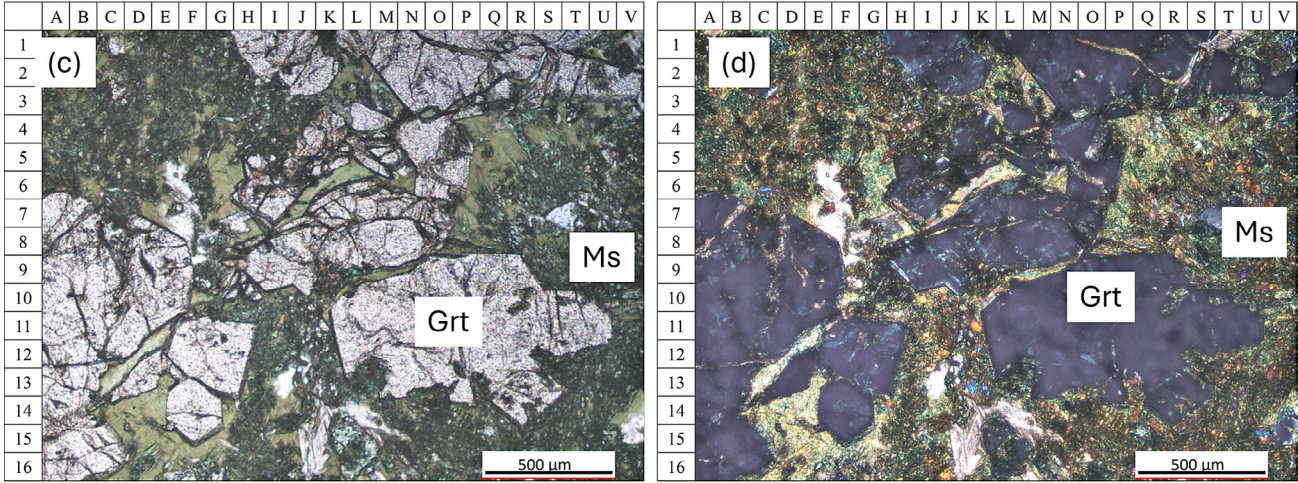


Figure 11. Altered garnet hand specimen marked with red box that locate thin section samples (a). Thin section samples from a hand specimen with a red circle that marks the microscope analysis (b). Photomicrograph of skarn mineralisation in Batubesi altered by late-stage mineralisation in parallel nicol (c) and cross nicol (d) from sample AB03002_A. Garnet is brecciated and altered to muscovite (G10). Abbreviations: Grt: garnet, Ms: muscovite

Skarn mineralisation in Batubesi is characterised by abundant magnetite, calc-silicate minerals, fluorite, muscovite, pyroxene, biotite, and amphibole. Magnetite is the most common skarn mineral found in the Batubesi deposit, with a black appearance and magnetic properties, commonly seen as a massive body, and layers found in wrigglite (see **Figure 9**) and alternating layers between magnetite and arsenopyrite. It becomes the main iron-bearing mineral in the Batubesi deposit. Magnetite is found to infill chalcedony in the deposit, then cut by a quartz vein, indicating their relative ages (see **Figure 10a**).

Calc-silicate minerals are typical minerals for skarn deposits. In the Batubesi deposit, calc-silicate minerals are commonly found as garnet, followed by wollastonite, vesuvianite, and actinolite. Garnet has a dull luster and different colours, such as red, green, and white, and is often found together with fluorite. Petrography analysis shows that garnet cut chalcedony mineral, indicating that garnet is younger than chalcedony (see **Figure 10c**). Garnet shows typical hexagonal structures with oscillatory zoning between isotropic and anisotropic parts. Many garnets were fractured and then underwent retrograde stage mineralisation, precipitating minerals such as biotite, amphibole, and muscovite (see **Figure 11**). The alteration sometimes is so intense that garnet is completely altered, retaining its oscillatory zoning features.

Wollastonite, actinolite, and vesuvianite are rarely found in the Batubesi deposit. Wollastonite can be found in an area with scarce calc-silicate or magnetite mineralisation, mostly unmineralized meta-siltstone (see Figure 8). It is primarily found in wollastonite-rich carbonate white layers with several metres thick, with cm to mm thick greenish pyroxene and fluorite-calcite veins (see Figure 12). Mineral sizes and habits are hard to determine by hand specimen observation as the sample has a uniform white colour. Petrography analysis suggests that the mineral habits are elongated parallel with a grey colour in parallel nicol and a grey to red-orange colour in cross nicol. On the other hand, actinolite and vesuvianite are rare and can be observed with garnet-rich rocks. Actinolite commonly occurs as an acicular mineral that has a pale green-green colour in parallel nicol and a greenish colour in cross nicol. Meanwhile, vesuvianite occurs as prismatic minerals in a thin section with high relief (similar with garnet), transparent in parallel nicol and grey (low birefringence) in cross nicol.

Ore minerals observed in the Batubesi area from petrographic analysis are cassiterite, magnetite, arsenopyrite, pyrite, and chalcopyrite that occur in skarn and as veins in meta-siltstone. Cassiterite mostly occurred in garnet-rich skarn mineralisation that have colourless to

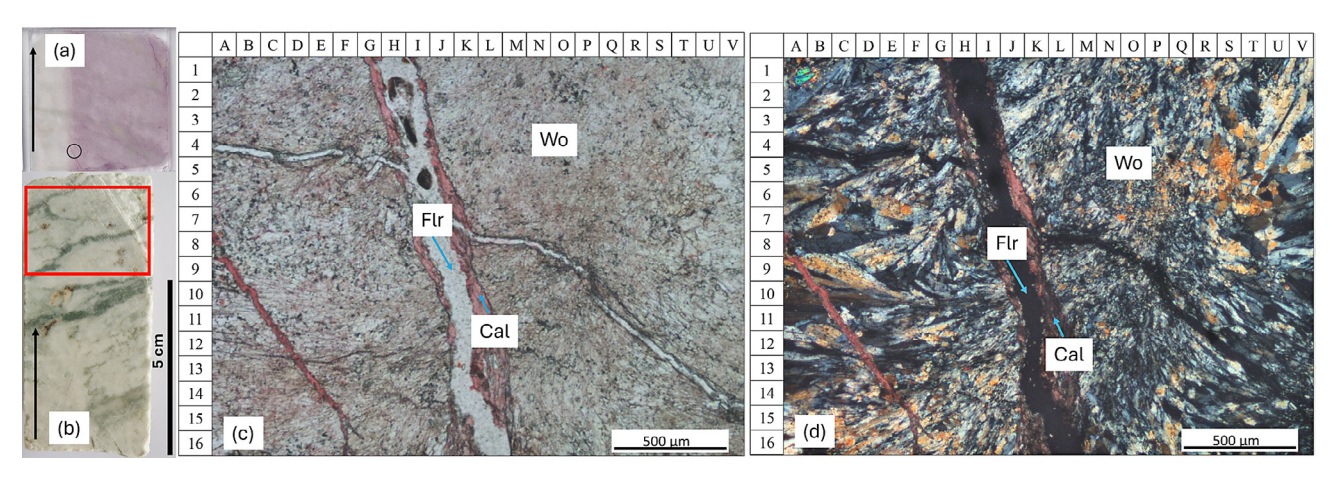


Figure 12. Wollastonite-rich rocks from ABo3014_B samples with red alizarin stain cut by calcite-fluorite veins with a black circle that shows the observation zone by optical microscope (a). Sample from drill core marked with a thin section region (b). Parallel nicol (c) and cross nicol (d) photomicrograph that shows wollastonite mineral cut by fluorite and calcite veins.

Abbreviations: Wo: wollastonite, Cal: calcite, Flr: fluorite

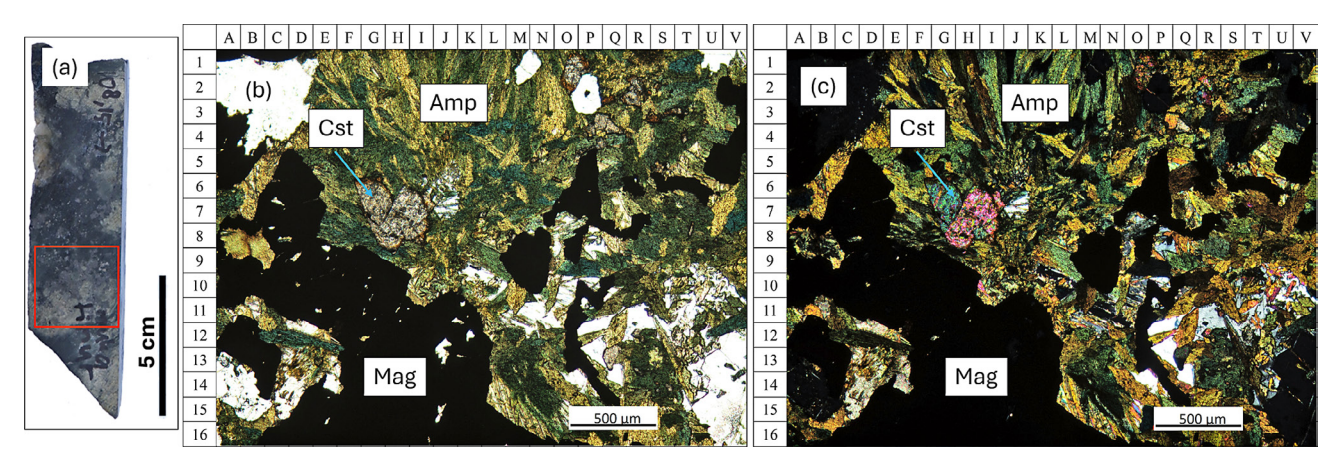


Figure 13. Location of thin section (red box) in core samples (a). Photomicrograph of cassiterite mineral in parallel nicol (brownish green, H7) (b) and cross nicol (green-pink, H7) (c) in Batubesi from sample ABo2032_B. Abbreviations:

Cst: cassiterite, Amp: amphibole, Mag: magnetite

brown colour in thin sections, with sizes from $160 \, \mu m$ to around $400 \, \mu m$ (see **Figure 13**). Some of them were found in altered garnets, while others were found in unaltered garnets. Magnetite can be seen as massive and layered mineral often shows wrigglite and fluid-like banded structure. Petrographic analysis in the wrigglite zone show that it comprises opaque minerals (mostly magnetite) and fluorite. On the other hand, in fluid-like banded structures opaque minerals mostly magnetite, with a minor amount of arsenopyrite, pyrite, and chalcopyrite.

3.2. XRD

X-ray diffraction analysis is usually coupled with petrographic analysis to determine mineral type in the study area. It is the primary mineral determination analysis for rocks that contain smaller minerals, such as meta-silt-stone. Based on XRD data coupled with petrographic analysis, meta-siltstone is composed of quartz, muscovite, and kaolinite (see **Figure 14**). Phlogopite, micro-

cline, albite, fluorite, magnetite, annite, pargasite, hastingsite, chamosite, andradite, uvarovite, vesuvianite, ferro-actinolite, cassiterite, and hedenbergite were also detected in XRD analysis.

3.3. *SEM-EDX*

SEM-EDX is useful to analyse minerals by their chemical composition. Despite its small area of analysis compared to micro-XRF, SEM-EDX successfully analyses light elements such as fluor and heavy elements such as wolfram. It is used for the identification of minerals that contain light elements (e.g. fluorite) as well as minerals that are too small to be identified by optical microscopes and their abundance is too small to be detected by bulk XRD analyses. Carbon contamination can be seen throughout the samples, because it can be found in magnetite and all other samples. It is caused by diamond paste during the polished sample preparation before the SEM-EDX analysis. This method analyses magnetite and fluorite bands in wrigglite, as well as other minerals such as

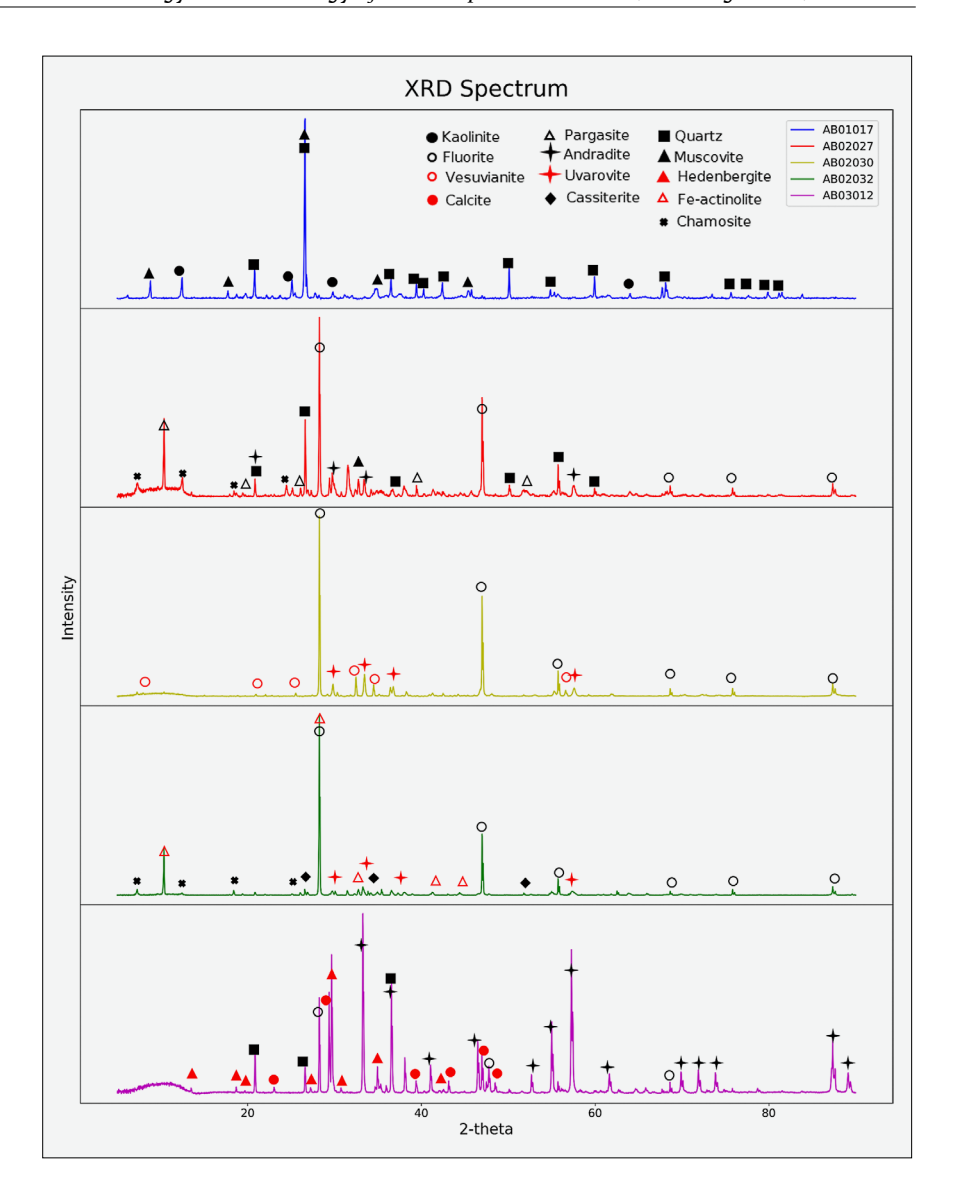


Figure 14. Bulk sample XRD spectrum of samples from Batubesi Fe-Sn deposit that shows various minerals from skarn and meta-siltstone

glaucocerinite, cassiterite, and scheelite by chemical mapping (see **Figure 15**). Additionally, point analysis shows that wolfram-bearing minerals in Batubesi are composed of ferberite and scheelite (see **Figure 16**). Scheelite are often found with a minor amount of ferberite, suggesting alteration occurs between W-bearing minerals.

3.4. Micro-XRF

Micro-XRF analysis shows that ore minerals detected in Batubesi region are magnetite, cassiterite, ferberite, scheelite, arsenopyrite, pyrite, chalcopyrite, and sphalerite. Cassiterite, ferberite, and scheelite mainly occur as fine minerals, ranging from 25 μm (one pixel) to 700 μm (see **Figure 17** and **Figure 18**). In addition, arsenopyrite, pyrite, and chalcopyrite can be seen in larger minerals, up to several millimetres. Arsenopyrite, pyrite, and chalcopyrite are commonly found as mineral assemblages (see **Figure 17**).

Hematite and pyrite veins are also present and detected by micro-XRF analysis. Hematite vein cut andradite mineral, with a small amount of Sn-bearing mineral. The analysis suggests that the Sn-bearing mineral is malayaite, but other possibilities (e.g. fine cassiterite) may be possible because of silica contamination from andradite during micro-XRF spot analysis. Conversely, pyrite veins are frequently shown with other sulphide minerals such as arsenopyrite and chalcopyrite. Later point analysis in garnet mineral shows that it contains a large amount of Fe, suggesting that it can be classified as andradite.

4. Discussion

4.1. Host rock characteristics

The characteristics of host rock play an important part in skarn mineralisation, as they can affect the redox and chemical characteristics of ore mineralisation, including skarn systems. The host rock in the Batubesi deposit is composed of sedimentary rocks, mainly siliciclastic rocks, with no carbonate present. Although not as common as its carbonate-hosted counterparts, siliciclastic skarn has been recorded previously (e.g. **Chang et al., 2019**).

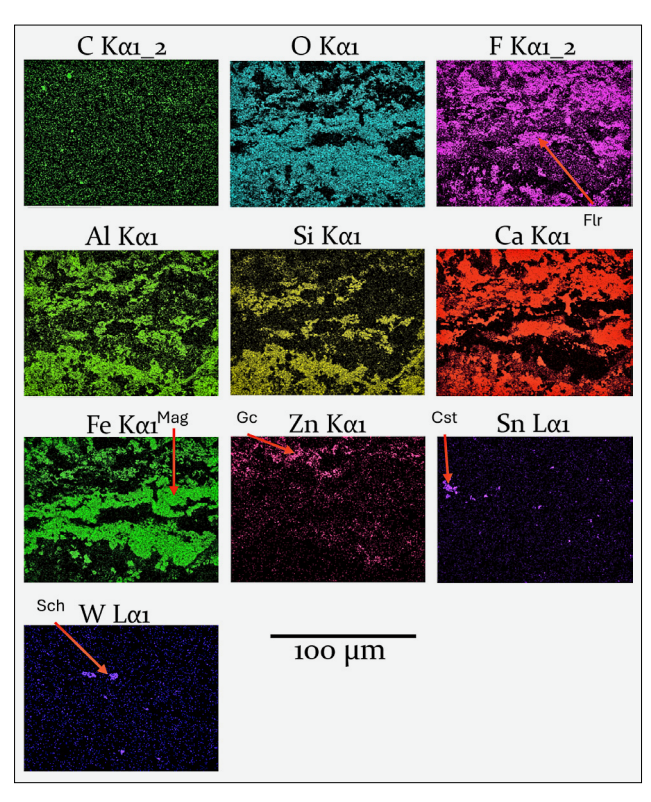


Figure 15. SEM-EDX analysis on wrigglite from skarn (ABo2013) shows magnetite and fluorite bands with small amounts of glaucocerinite, cassiterite, and scheelite (Fe, Sn, and W modified after Sugiharto et al., 2024). Abbreviations: Gc: glaucocerinite, Flr: fluorite, Mag: magnetite, Cst: cassoterite, Sch: scheelite

Meta-siltstone is observed near the sediment-granite contact, probably due to metamorphism caused by granitic intrusions, which is common in skarn-related mineralisation (**Pirajno**, 2008). It can also be seen in zones of highly mineralised skarn zones, and the amounts tend to increase outwards to the low mineralised skarn zones. Besides that, evidence of another type of rock is also

present in the area. Indications of another type of host rock are garnet and magnetite seen to be intruded and filled spaces between early minerals (chalcedony) in petrographic analysis (see Figure 10). Both minerals are commonly related to early skarn mineralisation (Chen et al., 2023; Lu et al., 2003; Mei et al., 2015), chalcedony probably comes from earlier rocks and does not correlate with Batubesi's meta-siltstone known characteristics. Despite that, the rock types and characteristics of chalcedony-bearing rocks remain unclear because it is largely replaced during skarn mineralisation.

4.2. Granitic rock

Plutonic igneous rocks in Belitung can be divided into four types, namely gabbroic, granodioritic, adamellitic, and granitic rocks (Aleva, 1960). However, later studies suggest that no gabbroic igneous rocks are present; only basaltic lava can be found (Baharuddin & Sidarto, 1995). Igneous rocks in the study area mainly comprise quartz and feldspar, with a small amount of biotite and zircon. It can be classified as felsic rocks and has a granitic composition. The granite is fine-grained and has equigranular to porphyry textures. Feldspar in granite commonly has a perthite structure. No vein is observed in granitic rocks, but fractures develop. Some of them have greisen alteration with plagioclase and feldspar are often altered to muscovite. Greisen alteration that occurs in granite related to skarn deposits is observed in other deposits that are products of the same mineralisation system as skarn (Meyer et al., 2024).

4.3. Alteration and mineralisation

Skarn mineralisation dominates the study area, with smaller amounts of greisen mineralisation near the granitic rocks. Skarn is characterised by calc-silicate and magnetite mineralisation that is several hundred meters wide and tens of meters deep. In contrast, greisen is characterised by quartz and muscovite-dominated rocks sev-

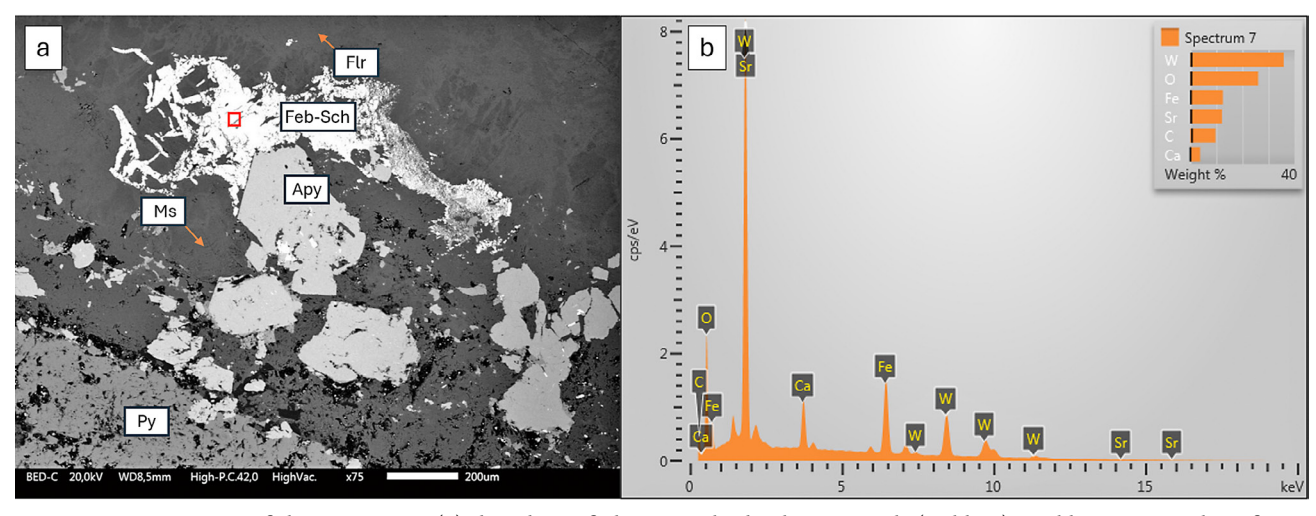


Figure 16. BSE image of skarn ABo2037 (a) that shows ferberite and scheelite minerals (red box). Red box EDX analysis from (a) shows that the composition is C, O, Ca, Fe, Sr, and W (b). Abbreviations: Apy: arsenopyrite, Py: pyrite, Feb: ferberite, Sch: scheelite, Ms: muscovite, Flr: fluorite

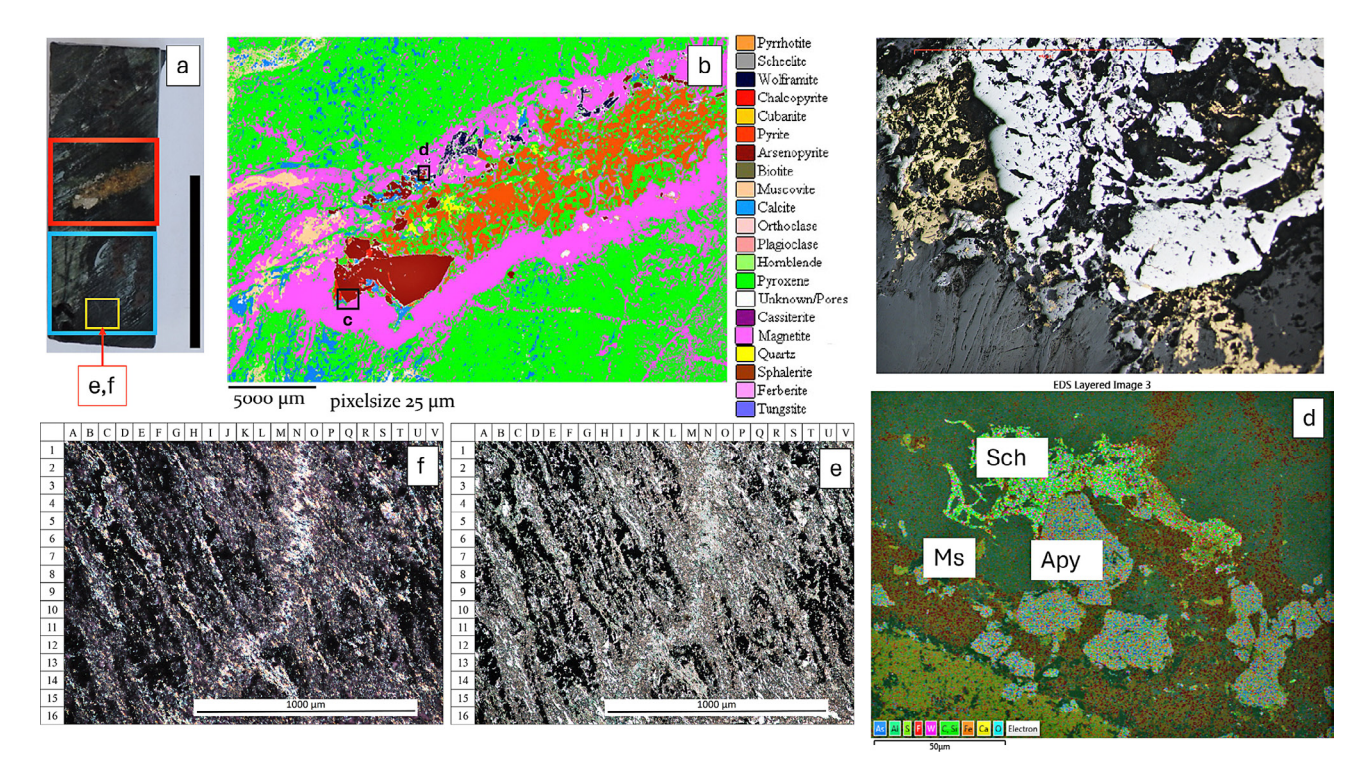


Figure 17. Multiple microanalysis to determine mineral assemblages in Batubesi skarn sample ABo2037A. Quarter diamond drill samples with annotation for polished section (red box), thin section (blue box), and photomicrograph (yellow box) (a). Micro-XRF analysis shows mineral assemblage in polished section with green is pyroxene, pink is magnetite, dark red is arsenopyrite, orange is pyroxene, and blue is wolframite (b). Petrographic analysis from the polished section shows arsenopyrite (grey) and chalcopyrite (dark yellow) (c). SEM-EDX analysis that shows scheelite (Sch), arsenopyrite (Apy), and muscovite (Ms) minerals (d). Parallel nicol (e) with cross nicol (f) photomicrograph from thin section that show layers of opaque (magnetite?) and translucent (muscovite?) minerals that are cut by a late muscovite vein

eral meters deep and wide. This is different from the previous study that stated mineralisation in the Batubesi area is greisen (Schwartz et al., 1995; Sujitno et al., 1981)

Skarn mineralisation in the Batubesi deposit is formed in meta-siltstone and chalcedony-bearing host rock, dominated by magnetite and garnet with minimal pyroxene present. The skarn mineralisation has three stages, similar to the skarn formation model from which is isochemical metamorphism, prograde skarn, and retrograde skarn (Pirajno, 2008). The retrograde skarn occurred in the brecciated (see Figure 11) or fractured lithology (see Figure 17). This is related to fluid flow and permeability of retrograde mineralising fluid in skarn.

Garnet is abundant in the Batubesi deposit compared to pyroxene. This ratio can inform us about the redox state during skarn mineralisation. Garnet is precipitated in an oxidised state, whereas pyroxene is precipitated in a reduced which is mainly controlled by element supply of ferric/ferrous element from skarn system (Chang & Meinert, 2008). Thus, skarn mineralisation in the Batubesi Fe-Sn deposit is in an oxidised state.

4.4. Mineral zonation

Skarn commonly shows mineral zonation patterns, both spatial and temporal, that can help in deposit exploration (Meinert, 1997). For example, one model suggests that mineral zonation in skarn reaction from pluton

to wall rock is garnet>pyroxene, pyroxene<garnet, wollastonite, and marble (Meinert et al., 2005). This zonation is applicable in skarn systems that have oxidising magma and reducing wall rock (Chang & Meinert, 2008). However, the Batubesi deposit is in an oxidised state, thus, the zonation is not applicable. For example, the wollastonite zone in the Batubesi deposit is not situated near host rock, it is rather located inside garnet mineralisation. Observable mineral zonation in Batubesi deposit is caused by the degree of alteration from retrograde stage. Highly altered zones are present in the alteration center that is located in the middle of the magnetite-garnet rich zone, and then the alteration degree gradually weakens outside. This is probably caused by the supply of fluids gradually lessen by proportional to the distance from the source.

4.5. Ore mineral assemblage

Ore minerals found in Batubesi region are oxide minerals (e.g. magnetite, cassiterite and ferberite), sulfate minerals (scheelite), and sulfides (pyrite, chalcopyrite, and arsenopyrite). Magnetite is the most abundant ore mineral in the Batubesi region that commonly has a massive structure; sometimes, it shows alternating layers with arsenopyrite. Magnetite cut by later carbonate, quartz, and sulfide veins shows that it precipitated early in the mineralisation process. Sulfide minerals in the Batubesi area are

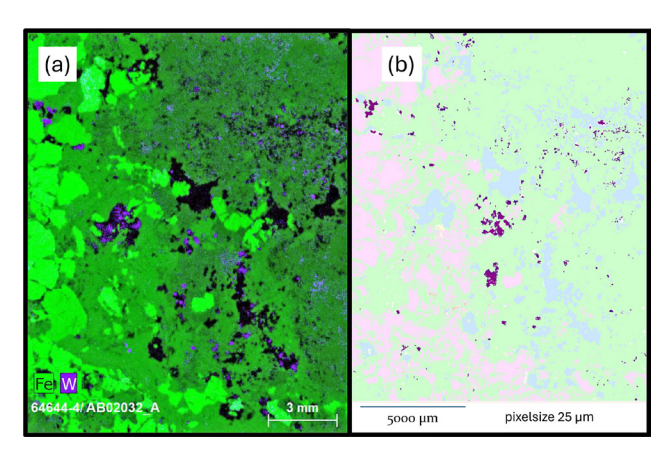


Figure 18. Wolfram element distribution from skarn sample ABo2o32_A (a) and Cassiterite mineral distribution (solid purple) in skarn sample ABo2o32_A (b). Other minerals in (b) are magnetite/ferberite (pink), pyroxene (green), and calcite (blue)

sometimes found as fine-grain minerals in magnetite. Still, they are commonly seen as sulfide veins in the latter skarn stage, ranging from several mm to several cm in widths composed of pyrite, chalcopyrite, and arsenopyrite. W-bearing minerals are only detected in SEM-EDX and micro-XRF as fine minerals. They are commonly found in similar grains, indicating that the minerals are altered. The alteration from scheelite to ferberite, and vice versa, is possible and controlled by several factors, such as the Ca/Fe ratio (**Baumer et al., 1985**).

5. Conclusions

Batubesi Fe-Sn deposit is one of the primary tin mineralisation in Belitung, known to have greisen-type mineralisation. Recently, skarn-type mineralisation has been known to develop in the region, but there is minimal information about it. This research has been done to study mineralisation in Batubesi, including the skarn-type mineralisation.

Host rock in Batubesi is composed of meta-siltstone and chalcedony-bearing rock, with no carbonate rocks present. Despite that, meta-siltstone is the one that is commonly found as a host rock in Batubesi. Minerals in the host rocks is around 12-23 µm consisting of quartz, muscovite, and kaolinite. Characteristics and composition of chalcedony-bearing rocks is not understood because the rocks are completely replaced with skarn-bearing rocks.

The Batubesi Fe-Sn deposit mineralisation type can be divided into skarn-type mineralisation and greisentype mineralisation. Greisen mineralisation occurs near granite intrusion with several meters thick, underlain skarn. Greisen is characterised by mineralisation of muscovite. Some of the muscovite can be found as the product of plagioclase and feldspar alteration.

Skarn mineralisation is several hundred meters thick and is characterised by calc-silicate and magnetite mineralisation. It can be divided into three stages: isochemical metamorphism, prograde and retrograde. Isochemical metamorphism is characterised by the development of meta-siltstone. Prograde skarn was identified as having calc-silicate and magnetite mineralisation. Magnetite is only present in the highly altered part of the skarn. Conversely, garnet commonly occurs in massive texture along with fluorite and is often brecciated or fractured and then filled with biotite, muscovite, and amphibole minerals from the retrograde stage. It is also cut by other minerals from the retrograde stage such as quartz, Feoxides (hematite), and carbonate veins with or without an alteration envelope. Additionally, the retrograde stage also consists of sulfide minerals, such as pyrite, chalcopyrite, and arsenopyrite.

Acknowledgement

We thank PT TIMAH for its permission and accommodations during sample collection and field observations, the National Research and Innovation Agency, Indonesia, for laboratory analysis, and the Faculty of Earth and Science and Technology, Institut Teknologi Bandung, for laboratory analysis. ADH would like to thank the Saintek Scholarship from the Ministry of Research and Technology National Research and Innovation Agency, which was continued by the National Research and Innovation Agency Continuing Scholarship during its doctoral study in Institut Teknologi Bandung.

Funding

This research was funded by the Saintek Scholarship from the Ministry of Research and Technology, National Research and Innovation Agency, followed by Continuing Scholarship from the National Research and Innovation Agency, Indonesia.

6. References

Adam, J. (1960). On the geology of the primary tin-ore deposits in the sedimentary formation of Billiton. *Geologie en Mijnbouw*, 39(10), 405-426.

Aleva, G. J. J. (1960). The plutonic rocks from Billiton. *Geologie en Mijnbouw*, 39(10), 427-436.

Baharuddin, & Sidarto (Cartographer). (1995). Peta Geologi Lembar Belitung, Sumatera

Bargawa, W. S., Sidiq, H., Dovena, A., & Supandi, S. (2023). Skarn and Greisen Model for Tin Depositin Batubesi Area, East Belitung, Indonesia. *The Iraqi Geological Journal*, 77-88.

Baumer, A., Caruba, R., & Guy, B. (1985). Experimental study of hydrothermal transformations scheelite≠ ferberite: preliminary results. *Bulletin de minéralogie*, 108(1), 15-20. doi:10.3406/bulmi.1985.7854

Chang, Z., & Meinert, L. D. (2008). Zonation in skarns - Complexities and controlling factors. In *Proceedings of PAC-RIM Congress 2008*. Goldcoast, Queensland, Australia.

Chang, Z., Shu, Q., & Meinert, L. (2019). Skarn Deposits of China. In *Mineral Deposits of China: Society of Economic Geologists Special Publication* (Vol. 22, pp. 189).

- Chen, S.-C., Yu, J.-J., Bi, M.-F., & Lehmann, B. (2022). Tinbearing minerals at the Furong tin deposit, South China: Implications for tin mineralization. *Geochemistry*, 82(1), 125856. doi:https://doi.org/10.1016/j.chemer.2021.125856
- Chen, Y.-K., Ni, P., Pan, J.-Y., Cui, J.-M., Li, W.-S., Fang, G.-J., Han, L. (2023). Fluid evolution and metallogenic mechanism of the Xianghualing skarn-type Sn deposit, South China: Evidence from petrography, fluid inclusions and trace-element composition of cassiterite. *Ore Geology Reviews*, 154, 105351. doi:https://doi.org/10.1016/j.ore-georev.2023.105351
- Cobbing, E. J., Mallick, D. I. J., Pitfield, P. E. J., & Teoh, L. H. (1986). The granites of the Southeast Asian Tin Belt. *Journal of the Geological Society*, 143(3), 537-550. doi:10.1144/gsjgs.143.3.0537
- Crow, M., & Van Leeuwen, T. (2005). Metallic mineral deposits. *Geological Society, London, Memoirs*, 31(1), 147-174.
- Dill, H. G. (2010). The "chessboard" classification scheme of mineral deposits: Mineralogy and geology from aluminum to zirconium. *Earth Science Reviews*, 100(1), 1-420. doi: 10.1016/j.earscirev.2009.10.011
- Einaudi, M. T., Meinert, L. D., Newberry, R. J., & Skinner, B.J. (1981). Skarn Deposits. In *Seventy-Fifth Anniversary Volume* (pp. 0): Society of Economic Geologists.
- Hutchison, C. S. (1978). Southeast Asian tin granitoids of contrasting tectonic setting. *Journal of Physics of the Earth*, 26(Supplement), S221-S232.
- Hutchison, C. S. (2014). Tectonic evolution of Southeast Asia. *Bulletin of the Geological Society of Malaysia, 60*, 1-18.
- Johari, S. (1987). Relationship between Sn mineralization and geochemical anomalies in non-residual overburden at Tebrong area, Belitung, Indonesia. *Journal of Geochemical Exploration*, 28(1-3), 219-234.
- Kunz, B. E., Warren, C. J., Jenner, F. E., Harris, N. B. W., & Argles, T. W. (2022). Critical metal enrichment in crustal melts: The role of metamorphic mica. *Geology*, 50(11), 1219-1223. doi:10.1130/g50284.1
- Lafuente, B., Downs, R. T., Yang, H., & Stone, N. (2016). The power of databases: the RRUFF project. In *Highlights in mineralogical crystallography* (pp. 1-29): Walter de Gruyter GmbH.
- Lehmann, B. (2020). Formation of tin ore deposits: A reassessment. *LITHOS*, 105756. doi:https://doi.org/10.1016/j. lithos.2020.105756
- Li, H., Qin, W., Li, J., Tian, Z., Jiao, F., & Yang, C. (2021). Tracing the global tin flow network: highly concentrated production and consumption. *Resources, Conservation* and *Recycling*, 169, 105495. doi:https://doi.org/10.1016/j. resconrec.2021.105495
- Lu, H.-Z., Liu, Y., Wang, C., Xu, Y., & Li, H. (2003). Mineralization and Fluid Inclusion Study of the Shizhuyuan W-Sn-Bi-Mo-F Skarn Deposit, Hunan Province, China. *Economic Geology*, 98(5), 955-974. doi:10.2113/gsecongeo.98.5.955
- Mei, W., Lü, X., Cao, X., Liu, Z., Zhao, Y., Ai, Z., . . . Abfaua, M. M. (2015). Ore genesis and hydrothermal evolution of the Huanggang skarn iron—tin polymetallic deposit, southern Great Xing'an Range: Evidence from fluid inclusions

- and isotope analyses. *Ore Geology Reviews*, 64, 239-252. doi:https://doi.org/10.1016/j.oregeorev.2014.07.015
- Meinert, L. D. (1992). Skarns and Skarn Deposits. *Geoscience Canada*, 19. doi:10.12789/gs.v19i4.3773
- Meinert, L. D. (1997). Application of skarn deposit zonation models to mineral exploration. *Exploration and Mining Geology*, 6, 185-208.
- Meinert, L. D. (2020). 3. The genesis and exploration of skarn deposits. *Geochemical Perspectives*, 9(1), 17-41.
- Meinert, L. D., Dipple, G. M., Nicolescu, S., Hedenquist, J. W., Thompson, J. F. H., Goldfarb, R. J., & Richards, J. P. (2005). World Skarn Deposits. In *One Hundredth Anniversary Volume* (pp. 0): Society of Economic Geologists.
- Metcalfe, I. (2017). Tectonic evolution of Sundaland. *Bulletin of the Geological Society of Malaysia*, 63, 27-60. doi: 10.7186/bgsm63201702
- Meyer, N., Markl, G., Gerdes, A., Gutzmer, J., & Burisch, M. (2024). Timing and origin of skarn-, greisen-, and veinhosted tin mineralization at Geyer, Erzgebirge (Germany). *Mineralium Deposita*, 59(1), 1-22. doi:10.1007/s00126-023-01194-8
- Moss, R., Tzimas, E., Willis, P., Arendorf, J., Thompson, P., Chapman, A., . . . Peason, J. (2013). Critical Metals in the Path towards the Decarbonisation of the EU Energy Sector. Assessing rare metals as supply-chain bottlenecks in low-carbon energy technologies. JRC Report EUR, 25994.
- Neymark, L. A., Holm-Denoma, C. S., Larin, A. M., Moscati, R. J., & Plotkina, Y. V. (2021). LA-ICPMS U-Pb dating reveals cassiterite inheritance in the Yazov granite, Eastern Siberia: Implications for tin mineralization. *Mineralium Deposita*. doi:10.1007/s00126-020-01038-9
- Ng, S. W.-P., Whitehouse, M. J., Roselee, M. H., Teschner, C., Murtadha, S., Oliver, G. J. H., . . . Chang, S.-C. (2017). Late Triassic granites from Bangka, Indonesia: A continuation of the Main Range granite province of the South-East Asian Tin Belt. *Journal of Asian Earth Sciences*, *138*, 548-561. doi:10.1016/j.jseaes.2017.03.002
- Pirajno, F. (2008). *Hydrothermal processes and mineral systems*: Springer Science & Business Media.
- Priem, H., Boelrijk, N., Hebeda, E., Verdurmen, E., Verschure, R., & Bon, E. (1975). Isotope geochronology in the Indonesian tin belt. *Geology Mijnbouw*, *54*(1), 61-70.
- Railsback, L. B. (2003). An earth scientist's periodic table of the elements and their ions. *Geology*, 31(9), 737-740. doi:10.1130/g19542.1
- Schwartz, M., Rajah, S., Askury, A., Putthapiban, P., & Djaswadi, S. (1995). The southeast Asian tin belt. *Earth-Science Reviews*, *38*(2-4), 95-293. doi:10.1016/0012-8252 (95)00004-T
- Schwartz, M., & Surjono. (1990). Greisenization and albitization at the Tikus tin-tungsten deposit, Belitung, Indonesia. *Economic Geology*, 85, 691-713. doi:10.2113/gsecongeo.85.4.691
- Searle, M., Whitehouse, M., Robb, L., Ghani, A., Hutchison, C., Sone, M., . . . Oliver, G. J. H. (2012). Tectonic evolution of the Sibumasu–Indochina terrane collision zone in Thailand and Malaysia: constraints from new U–Pb zircon chronology of SE Asian tin granitoids. *Journal of the Geological Society*, 169(4), 489-500.

- Sugiharto, M. S., Artyanto, A., Pratama, W. V., & Basuki, N. I. (2024). Tungsten-bearing mineral occurrences of Batubesi tin skarn deposits. *Bulletin of Geology* 8(2). Retrieved from https://www.buletingeologi.com/index.php/buletingeologi/article/view/395
- Sujitno, S., Ronojudo, A., & Timak, M. (1981). The occurrence of complex tin-iron ores in Belitung, Indonesia. Hasan, AH, Bin, H., van Wees. H.(Eds), Complex Tin Ores and Related Problems, 107-123.
- U.S. Geological Survey. (2022). *Mineral commodity summaries 2022* (2022). Retrieved from Reston, VA: http://pubs. er.usgs.gov/publication/mcs2022
- Wolf, M., Romer, R. L., Franz, L., & López-Moro, F. J. (2018). Tin in granitic melts: The role of melting temperature

- and protolith composition. *LITHOS*, *310-311*, 20-30. doi: https://doi.org/10.1016/j.lithos.2018.04.004
- Yang, J.-H., Zhou, M.-F., Hu, R.-Z., Zhong, H., Williams-Jones, A. E., Liu, L., . . . Mao, W. (2020). Granite-Related Tin Metallogenic Events and Key Controlling Factors in Peninsular Malaysia, Southeast Asia: New Insights from Cassiterite U-Pb Dating and Zircon Geochemistry. *Economic Geology*, 115(3), 581-601. doi:10.5382/econgeo.4736
- Zhao, P., Yuan, S., Williams-Jones, A. E., Romer, R. L., Yan, C., Song, S., & Mao, J. (2022). Temporal Separation of W and Sn Mineralization by Temperature-Controlled Incongruent Melting of a Single Protolith: Evidence from the Wangxianling Area, Nanling Region, South China. *Economic Geology*, 117(3), 667-682. doi:10.5382/econgeo.4902

SAŽETAK

Geologija i mineralogija Fe-Sn ležišta u Batubesiju, otok Belitung, Indonezija

Ležište Batubesi primarno je Fe-Sn ležište koje se nalazi u istočnome dijelu Belitunga u Indoneziji. Prvotno je mineralizacija bila poznata kao grajzen, ali nedavne studije pokazale su da se u regiji razvio tip ležišta skarn. Unatoč tome, mineralizacija skarna nije dobro istražena. Cilj je ovoga istraživanja proučiti Fe-Sn mineralizaciju u Batubesiju geološkim i mineraloškim metodama, primarno iz terenskih opažanja, nabušenih jezgara iz bušotina i uzoraka. Pritom su korištene petrološke analize, SEM-EDX, mikro-XRF i XRD analize u svrhu određivanja mineraloškoga sastava, kao i XRF na principu fuzije za određivanje geokemijskoga sastava ležišta. Rezultati pokazuju da u ležištu Batubesi dominira mineralizacija skarnskoga tipa s manjim udjelom grajzena. Uočene su dvije faze skarna: progradna i retrogradna. Progradne faze karakterizira taloženje kalcitno-silikatnih minerala i magnetita koji su često frakturirani ili brečirani. Pukotine i breče zatim se mijenjaju u okviru retrogradne faze te su sastavljene od amfibola, muskovita i biotita. Ponekad je promjena toliko intenzivna da je prethodna progradna faza potpuno izmijenjena. Nadalje, retrogradna faza sastoji se od sulfidnih minerala u obliku žila poput pirita, halkopirita i arsenopirita. Magnetit je uobičajeni rudni mineral, a slijede ga kasiterit, šelit, ferberit, pirit, halkopirit, arsenopirit, glaukokerinit i sfalerit.

Ključne riječi:

Batubesi, željezo-kositar, skarn, rudno ležište, mineralogija

Author's contribution

Aryo Dwi Handoko (Doctoral Candidate) conceptualization, data curation, formal analysis, investigation, methodology, project administration, resources, validation, visualization, writing – original draft and writing – review & editing. **Mochamad Slamet Sugiharto** (Geologist) resources, and validation. **Syafrizal** (Professor) supervision and writing – review & editing. **Benyamin Sapiie** (Professor) supervision and writing – review & editing.

All authors have read and agreed to the published version of the manuscript.